JOC Article

Giant Extended π-Conjugated Dendrimers Containing the 10,15-Dihydro-5*H*-diindeno[1,2-*a*;1′,2′-*c*]fluorene Chromophore: Synthesis, NMR Behaviors, Optical Properties, and Electroluminescence

Xiao-Yu Cao,[†] Xue-Hui Liu,[‡] Xing-Hua Zhou,[†] Yong Zhang,[§] Yang Jiang,[‡] Yong Cao,*[,§] Yu-Xin Cui,*[,‡] and Jian Pei*[,†]

The Key Laboratory of Bioorganic Chemistry and Molecular Engineering of Ministry of Education, College of Chemistry and Molecular Engineering, Peking University Healthy Science Centre, Peking University, Beijing 100871, China, and Institute of Polymer Optoelectronic Materials and Devices, South China University of Technology, Guangzhou 510640, China

jianpei@chem.pku.edu.cn

Received April 30, 2004

This paper reports the facile synthetic strategy of a series of novel π-conjugated dendrimers (**G0** and **G1**) based on 10,15-dihydro-5*H*-diindeno[1,2-*a*;1′,2′-*c*]fluorene (truxene) in which the benzene cores are generated "in-situ" from acetyl aromatics by the acid-promoted cyclotrimerizations. The unique NMR behaviors, physical properties, and electroluminescence device applications are also presented. Besides the purity, the structure, and the confirmation of the successful formation and isolation of desired compounds by clear assignments of every molecule by ^{1}H and ^{13}C and 2D NMR characterizations, several astonishing NMR behaviors have been observed in various solvents. For **1**, chemical shift values belonging to H-2′ of hexyl substituents move to the most upfield; however, such chemical shift values move from 0.48 to 0.85 ppm when pyridine-d_5 or benzene-d_6 is used as solvent. Our dendrimers as the emissive layers in organic light-emitting diodes gave blue-green light with an external quantum efficiency up to 0.16% both for **G0** and for **G1** in nitrogen, respectively, which exhibit unique electroluminescence spectra in comparison with their corresponding photoluminescence ones.

Introduction

Triggered by their well-defined, unique macromolecular structures and fascinating properties, considerable interest has been devoted recently to the design and synthesis of novel dendrimers and star-shaped molecules.[1] In particular, extended π-conjugated dendrimers and star-shaped molecules with definite nanometer sizes and intrinsic stiff nature have been proven to exhibit interesting electrical, optical, nonlinear optical, and electroluminescent properties for applications in electronic and photoelectronic devices including organic light-emitting diodes (OLEDs).[2] One of the important challenging goals of dendrimer chemistry is to develop new families of π-conjugated dendrimers with novel branches and cores, to investigate their physical and chemical properties, and to understand the structure−property relationship within such structures.

The convergent approach to these dendritic molecules provides greater structural control, a lower number of reactions at each growth step, and more structural purity and synthetic versatility than their divergent counterpart.[1h] Recently, several synthetic strategies have been used to construct extended π-conjugated dendrimers.[3] However, such methodologies employ the repetition of activation and coupling steps to access target molecules iteratively, which not only requires a massive excess of

[†] College of Chemistry and Molecular Engineering, Peking University.
[‡] Peking University Healthy Science Centre.
[§] South China University of Technology.

(1) (a) Newkome, G. R.; Moorefield, C. N.; Vögtle, F. *Dendritic Molecules: Concepts, Synthesis, Perspectives*; Wiley-VCH: Weinheim, Germany, 2002. (b) Fréchet, J. M. J.; Tomalia, D. A. *Dendrimers and Other Dendritic Polymers*, Wiley: Chichester, U.K., 2001. (d) *Dendrimers V: Functional and Hyperbranched Building Blocks, Photophysical Properties, Applications in Materials and Life Sciences*; Vögtle, F., Schalley, C. A., Eds.; Topics in Current Chemistry No. 228; Springer-Verlag: Berlin, 2003. (d) *Dendrimers IV: Metal Coordination, Self-Assembly, Catalysis*; Vögtle, F., Schalley, C. A., Eds.; Topics in Current Chemistry No. 217; Springer-Verlag: Berlin, 2001. (e) *Dendrimers III: Design, Dimension, Function*; Vögtle, F., Ed.; Topics in Current Chemistry No. 212;Springer-Verlag: Berlin, 2001. (f) *Dendrimers II: Architecture, Nanostructure and Supermolecular Chemistry*; Vögtle, F., Ed.; Topics in Current Chemistry No. 210; Springer-Verlag: Berlin, 2000. (g) *Dendrimers*; Vögtle, F., Ed.; Topics in Current Chemistry No. 197; Springer-Verlag: Berlin, 1998. (h) Grayson, S. M.; Fréchet, J. M. J. *Chem. Rev.* **2001**, *101*, 3819−3868. (i) Strohriegl, P.; Grazulevicius, J. V. *Adv. Mater.* **2002**, *14*, 1439−1452. (j) Thelakkat, M. *Macromol. Mater. Eng.* **2002**, *287*, 442−461.

(2) (a) Loi, S.; Butt, H. J.; Hampel, C.; Bauer, R.; Wiesler, U. M.; Müllen, K. *Langmuir* **2002**, *18*, 2398−2405. (b) Liu, D.; Zhang, H.; Grim, P. C. M.; De Feyter, S.; Wiesler, U.-M.; Berresheim, A. J.; Müllen, K.; De Schryver, F. C. *Langmuir* **2002**, *18*, 2385−2391. (c) Halim, M.; Samuel, I. D. W.; Pillow, J. N. G.; Monkman, A. P.; Burn, P. L. *Synth. Met.* **1999**, *102*, 1571−1574. (d) Halim, M.; Samuel, I. D. W.; Pillow, J. N. G.; Burn, P. L. *Synth. Met.* **1999**, *102*, 1113−1114. (e) Halim, M.; Pillow, J. N. G.; Samuel, I. D. W.; Burn, P. L. *Adv. Mater.* **1999**, *11*, 371−374. (f) Halim, M.; Pillow, J. N. G.; Samuel, I. D. W.; Burn, P. L. *Synth. Met.* **1999**, *102*, 922−923. (g) Wang, P. W.; Lui, Y. J.; Devadoss, C.; Bharathi, P.; Moore, J. S. *Adv. Mater.* **1996**, *8*, 237−241. (h) Tomalia, D. A.; Naylor, A. M.; Goddard, W. A., III. *Angew. Chem., Int. Ed. Engl.* **1990**, *29*, 138−175.

10.1021/jo049268p CCC: $27.50 © 2004 American Chemical Society
Published on Web 08/13/2004

one reactant but also inevitably generates partially substituted byproducts, making the purification troublesome. Moreover, the preparation of giant dendrimers is easily complicated by steric inhibition, resulting in sharply decreased yields.[1h] The cyclotrimerization reactions have provided a powerful strategy for the construction of a 1,3,5-trisubstitued benzene moiety or hexasubstituted (tris-annulated) benzenes,[4] which have become important building blocks for the synthesis of bowl-shaped polycyclic aromatic hydrocarbons[5] and the rational synthesis of C_{60},[6] starburst or star-shaped molecules,[7] liquid crystals, and C_3 tripods materials in asymmetric catalysis and chiral recognition.[8] The reaction involves the "in-situ" formation of the central benzene moiety by a triple aldolization and dehydration of 3 equiv of acetylaromatic molecules catalyzed by acids. It exhibits unique features including merely one reactant and one desired product (1,3,5-trisubstitued benzene) along with only a few of β-methylchalcone intermediate.

Due to their rigid planarized oligophenyl unit within the backbone as well as the possibility of facial functionalization at the methylene bridge, poly(9,9-dialkylfluroene), oligo(9,9-dialkylfluroene), and ladder-poly(*p*-phenylene) (LPPP) derivatives have been exhibited unique chemical and physical properties and emerged as the most promising light-emitting materials for organic light-emitting diodes (OLEDs).[9] Recently, we chose 10,15-dihydro-*5H*-diindeno[1,2-*a*;1′,2′-*c*]fluorene (truxene) as building block for novel π-conjugated star-shaped molecules and dendrimers (Chart 1).[10] Three fluroene moieties are *annulated* to afford a unique three-dimensional symmetric truxene moiety by sharing a central benzene ring (Chart 2). Investigation of their photophysical properties would give insight into the effect of delocalization through the benzene core in dendrimers and star-shaped molecules based on polycyclic aromatics. The synthesis and properties of star-shaped oligothiophenes-functionalized truxene derivatives was recently reported.[10a] These molecules represented oligothiophenes and were interesting in that they provided a model of interchromophore contacts not only in main-chain polychromophores such as polythiophenes but also in star-shaped π-conjugated molecules. However, a question of fundamental importance for dendrimers constructed by polycyclic aromatics with C_3 tripods concerns the extent of delocalization for the inter-ring state, since it plays a key role in determining the frequency and efficiency of emission and because it reflects the ability of large fragments to delocalize through the small core.

In this paper, we first investigate the effects of various conditions, such as the concentration of hydrogen chlo-

CHART 1

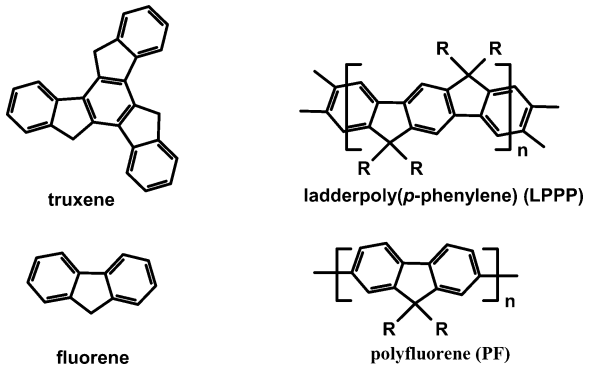

CHART 2

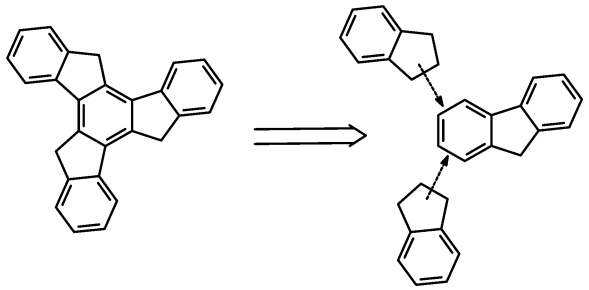

(3) For reported extended π-conjugated dendrimers, see: (a) Berresheim, A. J.; Müller, M.; Müllen, K. *Chem. Rev.* **1999**, *99*, 1747−1785. (b) Morgenroth, F.; Reuther, E.; Müllen, K. *Angew. Chem., Int. Ed. Engl.* **1997**, *36*, 631−634. (c) Moore, J. S. *Acc. Chem. Res.* **1997**, *30*, 402−413. (d) Devadoss, C.; Bharathi, P.; Moore, J. S. *J. Am. Chem. Soc.* **1996**, *118*, 9635−9644. (e) Gong, L.; Hu, Q.-S.; Pu, L. *J. Org. Chem.* **2001**, *66*, 2358−2367. (f) Meier, H.; Lehmann, M. *Angew. Chem., Int. Ed.* **1998**, *37*, 643−645. (g) Lupton, J. M.; Samuel, I. D. W.; Beavington, R.; Burn, P. L.; Bassler, H. *Adv. Mater.* **2001**, *13*, 258−261. (h) Deb, S. K.; Maddux, T. M.; Yu, L. *J. Am. Chem. Soc.* **1997**, *119*, 9079−9080. (i) Higuchi, M.; Shiki, S.; Ariga, K.; Yamamoto, K. *J. Am. Chem. Soc.* **2001**, *123*, 4414−4420. (j) Yamamoto, K.; Higuchi, M.; Shiki, S.; Tsuruta, M.; Chiba H. *Nature* **2002**, *415*, 509−511. (k) Xia, C.; Fan, X.; Locklin, J.; Advincula, R. C. *Org. Lett.* **2002**, *4*, 2067−2070. (l) Stocker, W.; Karakaya, B.; Schürmann, B. L.; Rabe, J. P.; Schlüter, A. D. *J. Am. Chem. Soc.* **1998**, *120*, 7691−7695. (m) Bo, Z.; Rabe, J. P.; Schlüter, A. D. *Angew. Chem., Int. Ed.* **1999**, *38*, 2370−2372. (n) Schlüter, A. D.; Rabe, J. P. *Angew. Chem., Int. Ed.* **2000**, *39*, 864−883.

(4) (a) Elmorsy, S. S.; Pelter, A.; Smith, K. *Tetrahedron Lett.* **1991**, *32*, 4175. (b) Plater, M. J. *Synth. Lett.* **1993**, *6*, 405−406. (c) Scott, L. T. In *Modern Arene Chemistry*; Astruc, D., Ed.; Wiley: Berlin, 2002. (d) Elmorsy, S. S.; Khalil, A. G. M.; Girges, M. M.; Salama, T. A. *J. Chem. Res., Synop.* **1997**, 232−233; *J. Chem. Res., Miniprint* **1997**, 1537−1544.

(5) (a) Gómez-Lor, B.; de Frutos, Ó.; Echavarren, A. M. *Chem. Commun.* **1999**, 2431−2432. (b) Mehta, G.; Rao, H. S. P. *Tetrahedron* **1998**, *54*, 13325-13370. (c) Ansems, R. B. M.; Scott, L. T. *J. Am. Chem. Soc.* **2000**, *122*, 2719−2724. (d) Rabideau, P. W.; Abdourazak, A. H.; Marcinow, Z.; Sygula, R.; Sygula, A. *J. Am. Chem. Soc.* **1995**, *117*, 6410−6411. (e) Sygula, A.; Rabideau, P. W. *J. Am. Chem. Soc.* **2000**, *122*, 6323−6324.

(6) (a) Boorum, M. M.; Vasil'ev, Y. V.; Drewello, T.; Scott, L. T. *Science* **2001**, *294*, 828−831. (b) Scott, L. T.; Boorum, M. M.; McMahon, B. J.; Hagen, S.; Mack, J.; Blank, J.; Wegner, H.; de Meijere, A. *Science* **2002**, *295*, 1500−1503.

(7) (a) Cherioux, F.; Guyard, L.; *Adv. Funct. Mater.* **2001**, *11*, 305−309. (b) Zhou, X.-H.; Yan, J.-C.; Pei, J. *Org. Lett.* **2003**, *5*, 3543−3546.

(8) (a) Dijkstra, H. P.; Kruithof, C. A.; Ronde, N.; van de Coevering, R.; Ramón, D. J.; Vogt, D.; van Klink, G. P. M.; van Koten, G. *J. Org. Chem.* **2003**, *68*, 675−685. (b) Lambert, C.; Nöll, G.; Schämlzlin, E.; Meerholz, K.; Bräuchle, C. *Chem. Eur. J.* **1998**, *4*, 2129−2135. (c) Perova, T. S.; Vij, J. K. *Adv. Mater.* **1995**, *7*, 919−922. (d) Fontes, E.; Heiney, P. A.; Ohba, M.; Haseltine, J. N.; Smith, A. B. *Phys. Rev. A* **1988**, *37*, 1329−1334. (e) Destrade, C.; Malthete, J.; Tinh, N. H.; Gasparoux, H. *Phys. Lett.* **1980**, *78A*, 82−84.

(9) (a) Grell, M.; Bradley, D. D. C.; Ungar, G.; Hill, J.; Whitehead, K. S.; *Macromolecules* **1999**, *32*, 5810−5187. (d) Jenekhe, S. A.; Osaheni, J. A. *Science* **1994**, *265*, 765. (b) Scherf, U.; List, E. J. M. *Adv. Mater.* **2002**, *14*, 477−487. (c) Setayesh, S.; Grimsdale, A. C.; Weil, T.; Enkelmann, V.; Müllen, K.; Meghdadi, F.; List, E. J. W.; Leising, G. *J. Am. Chem. Soc.* **2001**, *123*, 946−953. (d) Marsitzky, D.; Scott, J. C.; Chen, J.-P.; Lee, V. Y.; Miller, R. D.; Setayesh, S.; Müllen, K. *Adv. Mater.* **2001**, *13*, 1096−1099.

(10) (a) Pei, J.; Wang, J.-L.; Cao, X.-Y.; Zhou, X.-H.; Zhang, W.-B. *J. Am. Chem. Soc.* **2003**, *125*, 9944−9945. (b) Cao, X.-Y.; Zhang, W.-B.; Wang, J.-L.; Zhou, X.-H.; Lu, H.,; Pei, J. *J. Am. Chem. Soc.* **2003**, *125*, 12430−12431. (c) Chen, H.; He, M.-Y.; Cao, X.-Y.; Zhou, X.-H.; Pei, J. *Rapid. Commun. Mass. Spectrom.* **2004**, *18*, 367−370. (d) Gómez-Lor, B.; de Frutos, Ó.; Ceballos, P. A.; Granier, T.; Echavarren, A. M. *Eur. J. Org. Chem.* **2001**, *11*, 2107−2114. (e) de Frutos, Ó.; Granier, T.; Gómez-Lor, B.; Jiménez-Barbero, J.; Monge, M. Á.; Gutiérrez-Puebla, E.; Echavarren, A. M. *Chem. Eur. J.* **2002**, *8*, 2879−2890. (f) Ruiz, M.; Gómez-Lor, Santos, A.; Echavarren, A. M. *Eur. J. Org. Chem.* **2004**, 858−866.

SCHEME 1. Cyclotrimerization of Acetyl Aromatics

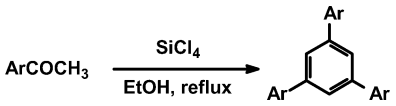

TABLE 1. Acid-Promoted Cyclotrimerization of Acetyl Aromatics

Entry 1	Ar	Yield
1		32 %[a]
2	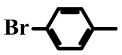	49 %[a]
3	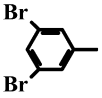	49 %[a]
4		< 10 %[b]
5	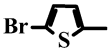	< 10 %[b]
6	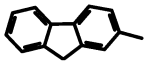	55 %[a]
7	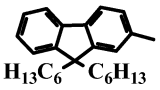	87 %[b]

[a] After recrystalization. [b] After flash chromatography. [c] 5 equiv of $SiCl_4$.

ride, the solubility of starting materials, and the amount of tetrachlorosilane ($SiCl_4$) on the acid-promoted cyclotrimerizations. Based on these results, we have successfully synthesized some extended π-conjugated dendrimers and star-shaped molecules with good yields, including the largest one based on truxene containing up to nine truxene moieties. Besides the standard characterization by the elemental analysis data, MALDI-TOF/MS measurement, and the absorption and emission spectra,[10b,c] we employed ^1H and ^{13}C and 2D NMR (COSY, HMBC, HSQC, and ROESY) techniques to characterize the structure and the conformation of our dendrimers in various solvents. The investigation of absorption and emission properties of the dendrimers in THF solutions and in the films indicated that the torsion angle between the benzene ring and truxene skeleton might play a key role on optical and physical properties. The dendrimers were also fabricated as the emissive layers in OLEDs.

Results and Discussion

Reaction Conditions Investigation. Our first strategy was to investigate the effect of the intrinsic solubility of all molecules on the reactions as shown in Scheme 1. In Table 1, the poor solubility of reactants and products resulted in relatively low yields, large amounts of starting materials, and tedious purification procedures (entries 1−6). In contrast, the introduction of two hexyl groups in the fluorene moiety not only greatly elevated the yield of the desired product but also significantly facilitated the isolation procedure (entry 7). Therefore, it provided

TABLE 2. Comparison with Conditions of Cyclotrimerizations to Dendrimer G0

entry	conditions[a]	yield[b] (%)
1	HOAc−HCl, 120 °C	NR
2	$SiCl_4$ (5 equiv), EtOH, reflux	<1
3	$SiCl_4$ (20 equiv), EtOH-Tol, reflux	23
4	$TiCl_4$ (1.5 equiv), o-$C_6H_4Cl_2$, 180 °C	100[c]
5	$TiCl_4$ (1.5 equiv), o-$C_6H_4Cl_2$, 140 °C	NR
6	$SiCl_4$ (30 equiv), $(HOC_2H_4)_2O$-Tol, 160 °C	12
7	$SiCl_4$ (20 equiv), EtOH-Tol, Et_3N, reflux	*d*
8	$SiCl_4$ (30 equiv), EtOH-Tol, reflux	91

[a] 24 h. [b] After purification. [c] Conversion. [d] A β-methylchalcone dimer was formed.

a strategy to access functional organic materials (especially like polycyclic aromatic hydrocarbons assembly) efficiently and conveniently. We deemed it constructive to extend our studies to a larger moiety with a polycyclic aromatic hydrocarbon framework. The heptacyclic polyarene truxene moiety, by virtue of its unique three-dimensional topology, is an attractive building motif for use as a potential dendrimer building block. However, the poor solubility and the large steric hindrance rendered the synthesis of these types of dendrimers a challenge. With the strategy presented above, we introduced six hexyl groups onto the C-5, C-10, and C-15 positions of the truxene moiety, which greatly enhanced the solubility and made the subsequent modification at C-2, C-7, C-12 positions by aromatic electrophilic substitution more facile.

However, the cyclotrimerizations of **G0** met severe difficulties due to the steric hindrance of the giant truxene moiety at first, which naturally forced us to further study the reaction. Table 2 summarizes the results under the various conditions. Initially, we attempted to afford **G0** by literature procedures (entries 1 and 2).[4] Although the addition of toluene could increase the yields of cyclotrimerizations (entry 3),[7a,8a] it is far from enough for some target molecules with giant substituted aromatic groups since good intrinsic solubility is a required criteria for both acquiring them and processing them into organic photoelectronic devices.

However, it reminded us that the solubility was not the most significant driving force to get across the steric hindrance barrier. We noticed the $TiCl_4$−dichlorobenzene system developed by Scott,[6] which turned out to be the most powerful strategy to convert **2** into **G0** molecule. However, we failed to exclude the dark black impurities from our products by all means of methods (entry 4). We also found it to be a temperature-dependent reaction. When the temperature decreased from 180 to 140 °C, the yield dropped dramatically from quantitative to none, and even the β-methylchalcone was not formed at this temperature (entry 5). It seems that such $TiCl_4$-dichlorobenzene system is more practical to those molecules with poor solubility.

Entry 7 revealed that the concentration of hydrogen chloride played a pivotal role in this reaction. No target compound was obtained when Et_3N was added; instead, quite a lot of β-methylchalcone was formed under this condition. Although the synthesis of β-methylchalcone with small aromatic substituents by using 1 equiv of $SiCl_4$ has been reported before,[4d] we developed an alternative method to prepare such compounds with giant aromatic substituents efficiently by both increasing the amount

SCHEME 2. Preparation of Dendrimers G0 and G1

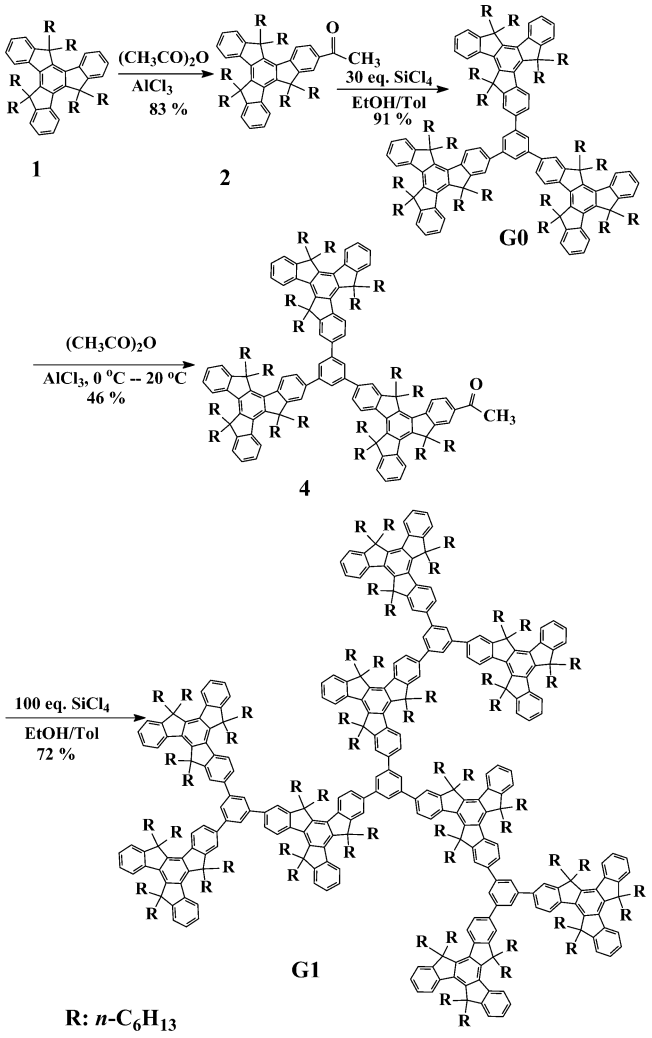

of $SiCl_4$ and addition of Et_3N to eliminate the hydrogen chloride in the system, which forced the reaction staying in the β-methylchalcone intermediate. Finally, we varied the amount of $SiCl_4$ from 20 to 30 equiv (entry 8), and the yields increased dramatically under this tendency.

Encouraged by such results, we decided to expand the scope of this strategy to a more ambitious level. With increasing the amount of $SiCl_4$ to 100 equiv, we even successfully prepared **G1**, a larger extended π-conjugated dendrimer based on truxene, by repetitive Friedel−Crafts acetylation and cyclotrimerizations (Scheme 2).[10b] Considering the rigid nature and severe steric hindrance of **G1**, the yield (72%) was quite remarkable after flash column chromatography. The transformation from acetyl aromatics to 1,3,5-trisubstituted benzenes was relatively clean, thus rendering the purification of the desired products quite simple by column chromatography. All compounds have been fully characterized by ^1H and ^{13}C NMR, elemental analyses, and MALDI-TOF MS.[10b,c]

NMR Behaviors and Molecular Modeling. The monodispersity and high symmetry associated with dendrimers have presented numbers of interesting characterization traits and obtained an unprecedented amount of the structural information utilizing advanced characterization techniques.[11] ^1H and ^{13}C NMR spectra allowed the identification of every unique proton or carbon atom

CHART 3. Numbering System Used for Discussion of Aromatic Framework and of Hexyl Side Chains[a]

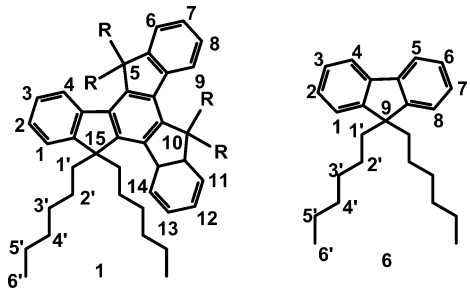

[a] The carbon atoms and corresponding hydrogen atoms were numbered the same, R = n-C_6H_{13}.

in the structure of some dendrimers, which could be used to help establish the purity of dendrimers as well as to provide an extremely related structural information.[12] In our previous report,[10a] we reported that ^1H NMR spectra of **1** and its oligothiophenes-functionalized derivatives in $CDCl_3$ did not exhibit any change with an increase of the concentration, indicating that the stretching long substituents effectively reduced self-association by arene π−π stacking.[10d,e] More surprisingly, the chemical shifts belonging to methylene groups moved more upfield than those of methyl groups, the values (about 0.5−0.6 ppm!) were considerably lower than those of methyl and other methylene groups. What is more, when we turned to a more extended scope, we found this astonishing behavior has actually also been existed in the extensively investigated 9,9-dialkylfluroene moiety.[13] By contrast with the extensive NMR investigation toward annulenes,[14] these perspective building blocks in materials science receive fairly little attention in this aspect. To shed light on such astonishing behavior and to better understand the aromaticity, the effective conjugation length, the conformation, and structure of dendrimers, we carried out a more detailed investigation by employing ^1H and ^{13}C and 2D NMR techniques. For the purpose of discussion, the carbon atoms and the corresponding hydrogen atoms were numbered the same. The aromatic framework (truxene, fluorene, and benzene moieties) and hexyl side chains were labeled in two numbering systems, starting from 1 and 1′, respectively (as shown in Chart 3).

The truxene and fluorene moieties (**1** and **6**) were served as models to understand the structure of the dendrimers (Figure 1). It is obvious that chemical shift values belonging to protons of one methylene group for both **1** and **6** moved more upfield. Distinct difference in resonance signals of H-1′ was also observed for these two compounds: only one group of multiplet peaks appeared

(11) (a) Hawker, C. J. *Advances in Polymer Science 147*; Springer-Verlag: Berlin, Heidelberg, Germany, 1999; pp 114−160. (b) Walker, K. L.; Kahr, M. S.; Wilkins, C. L.; Xu, Z.; Moore, J. S. *J. Am. Soc. Mass. Spectrom* **1994**, *5*, 731−739. (c) Leon, J. W.; Fréchet, J. M. J. *Polym. Bull.* **1995**, *35*, 449−455.

(12) Hawker, C. J.; Fréchet, J. M. J.*J. Am. Chem. Soc.* **1990**, *112*, 7638−7647.

(13) (a) Ranger, M.; Leclerc, M. *Macromolecules* **1999**, *32*, 3306−3313. (b) Destri, S.; Pasini, M.; Botta, C.; Porzio, W.; Bertini, F.; Marchiò, L. *J. Mater. Chem.* **2002**, *12*, 924−933. (c) Alder, R. W.; Anderson, K. R.; Benjes, P. A.; Burts, C. P.; Koutentis, P. A.; Orpen, A. G. *J. Chem. Soc., Chem. Commun.* **1998**, 309−310. (d) Ranger, M.; Bélanger-Gariépy, F.; Leclerc, M. *Acta Crystallogr., Part C* **1998**, *C54*, 799−805.

(14) Mitchell, R. H. *Chem. Rev.* **2001**, *101*, 1301−1315.

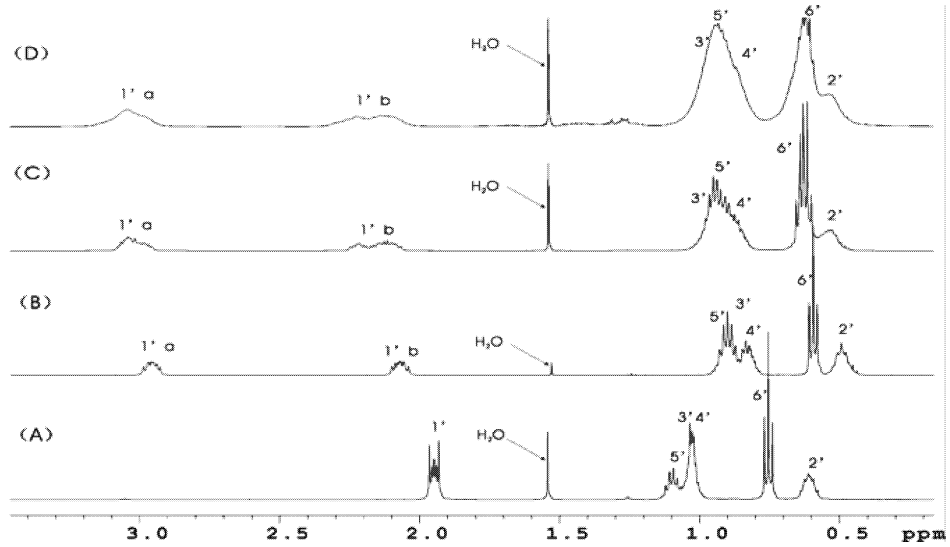

FIGURE 1. ^{1}H NMR spectra of (A) **6**, (B) **1**, (C) **G0**, and (D) **G1** at aliphatic regions in $CDCl_3$.

at 1.95 ppm for **6**; however, two groups of multiplet peaks exhibited at about 2.97 and 2.05 ppm for **1**, respectively. All chemical shift values of H2′−6′ in **1** moved to upfield in comparison with those of **6**. Meantime, as in **G0** and **G1**, the corresponding values continued slightly moving to downfield and the peaks became broad with the increase of the generation of dendrimers. 2D ^{1}H−^{1}H COSY, ^{1}H−^{13}C HSQC, ^{1}H−^{1}H ROESY, and ^{1}H−^{13}C HMBC results also demonstrated the same results (see the Supporting Information).

To better elucidate these interesting behaviors, the energy-minimized structures of 1 and 6 have been obtained employing the MM2 (MM+) force field optimization, as implemented in HyperChem Pro. 7.0 (Hypercube Inc.) (as shown in Figure 2). Due to the prohibitively large number of atoms in the subsequent dendrimers, a force field method was favored rather than quantum mechanics methods. The conformation of the resulting fluorene moiety (6) is in good agreement with that of the reported crystal structure analysis, in which the all-anti alkyl side chains in 9,9-dialkylfluorene are orthogonally stretched to the fluorene ring plane.[13b−d] As a result, it would be safely to assume that the calculated structures of its three-direction analogue truxene moiety (1) and dendrimers (G0 and G1) are as good an approximation as the fluorene model is. The substituted truxene moiety displayed similar side chains conformation as the fluorene segment from the view of the lowest-energy structure calculation. The optimized structure of 1 was also employed to build up its dendrimer derivatives G0, and then the energy-minimized structure of G0 was employed to build up larger dendrimer G1. After rotation around the three bonds connecting the truxene moiety (or the G0 subunit) and central benzene, several conformations were obtained. The conformations with lowest energy for the dendrimers G0 and G1 were shown in Figure 3.

The above^{1}H NMR behaviors could be interpreted by traditional ring current model based on the "Pauling−Lonsdale−London π model".[15] The shielding and deshielding regions are inside or outside the anisotropic cones induced by the intramolecular ring currents in our aromatic frameworks, either the truxene moiety or the fluorene moiety. The shielding effect vanishes with increasing distance from the ring along the molecular axis. As shown in Figure 2, all hexyl substituents in **1** and **6** are almost perpendicularly attached to the aromatic ring plane, and the H-2′ suffered the most severe upfield shift because they were situated in the shielding cone of the aromatic ring. Since the shielding effect decreased with increasing distance from the ring along the molecular axis, the H-4′ signals shifted downfield in comparison with those of H-2′. Likewise, due to the shielding effect difference between their locations, the H-2′, H-4′, and H-6′ were more shielded than corresponding H-1′, H-3′, and H-5′, respectively. The different H-1′ signals of **1** and **6** could be ascribed to the different chemical environment surrounding them.

With these data in hand, to further understand the relationship between the NMR and the structure and also to investigate the effect of the hexyl substituents on the conformation of the whole molecule, we investigated the ^{1}H and ^{13}C NMR behaviors by varying the solvents. When the solvent was changed from $CDCl_3$ to pyridine-d_5 or benzene-d_6, we observed that chemical shift values of all protons at hexyl substituents moved to downfield, especially abnormal chemical shift ones of H-2′ moved to the downfield from 0.48 to 0.75 ppm, and chemical shift ones of methyl groups also moved about 0.05 ppm. Figure 7 presents the comparison of the ^{1}H NMR spectra of **1** in different solvents (as shown in Figure 4). The similar behavior was also observed for the ^{1}H NMR spectra of **6** (see the Supporting Information).

Although the polar $CDCl_3$ molecule can have electrostatic interactions with a polar substrate, it can only interact with nonpolar molecules **1** or **6** through van der Waals forces and had a minimal effect on the chemical shift value. On the other hand, the disklike benzene or pyridine molecule possessed large diamagnetic anisotropy, hence resulting in an upfield shift (decrease of chemical shift value). We assumed that the disklike

(15) Gomes, J. A. N. F.; Mallion, R. B. *Chem. Rev.* **2001**, *101*, 1349−1384.

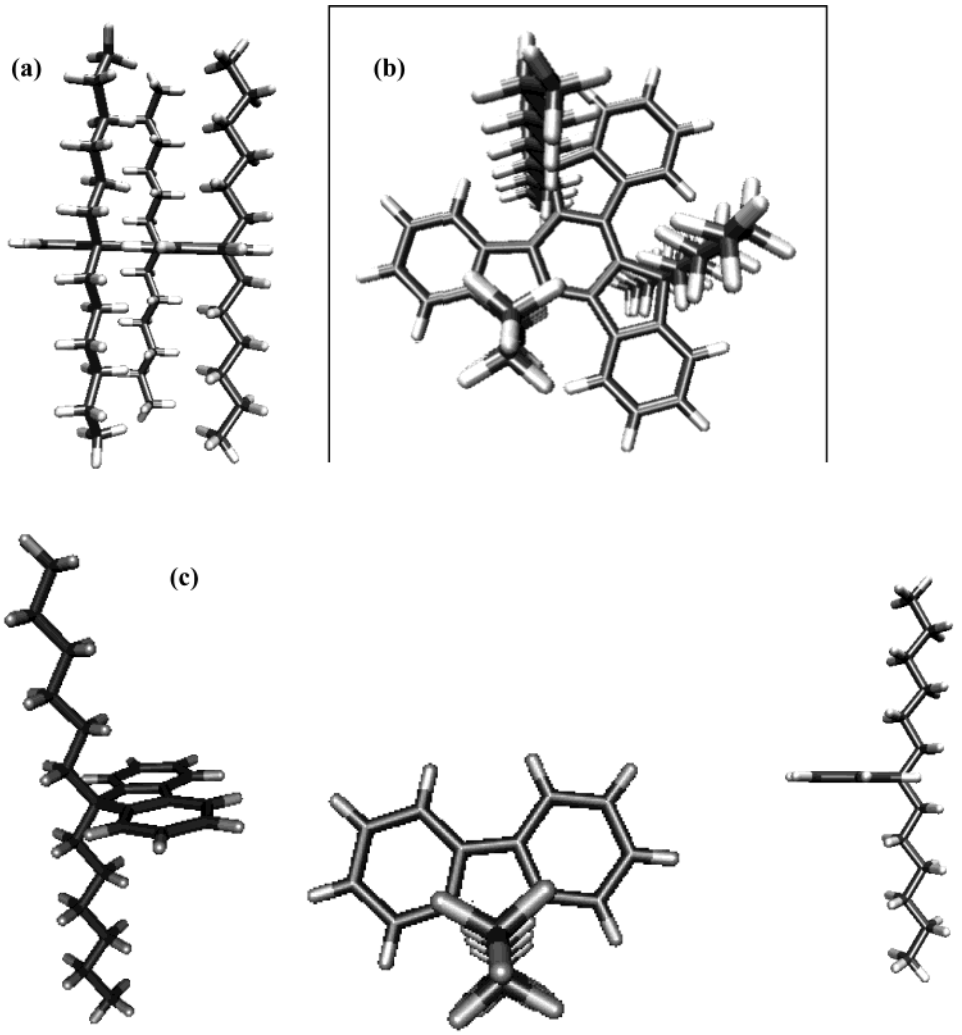

FIGURE 2. Lowest energy calculated structures of the front (a) and side view (b) for **1** and of the front view for **6** (c).

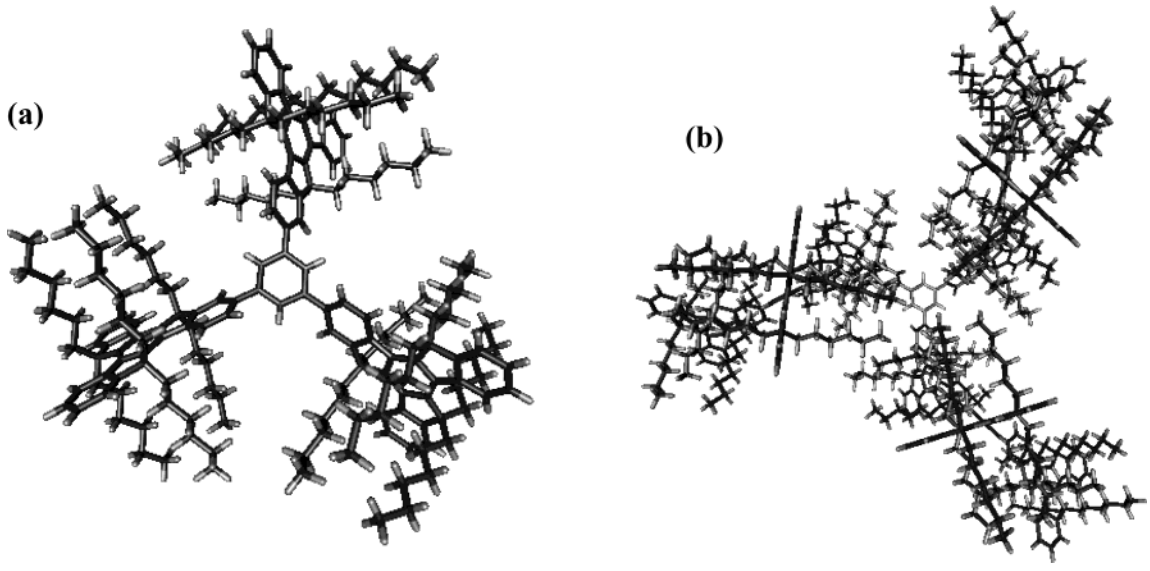

FIGURE 3. Lowest energy calculated structure for **G0** (a) and **G1** (b).

aromatic solvent molecules interacted with the substrate by $\pi-\pi$ stacking. As a consequence, the H-2′ and some other protons were exposed to the deshielding regions of the solvent molecules, which would attenuate the shielding effect from the substrate aromatic frameworks. It is well-known that the accidentally overlapping resonance

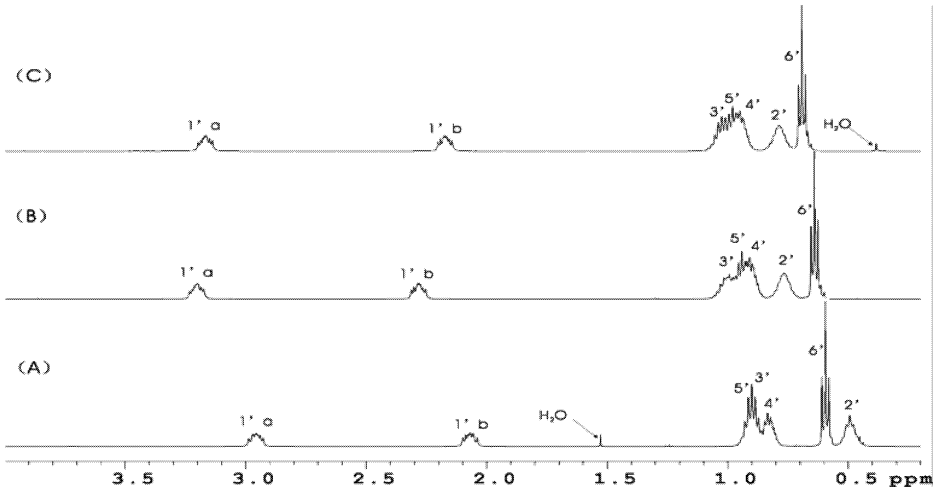

FIGURE 4. ^{1}H NMR spectrum of **1** (lower) in (A) $CDCl_3$, (B) pyridine-d_5, and (C) benzene-d_6 solvent.

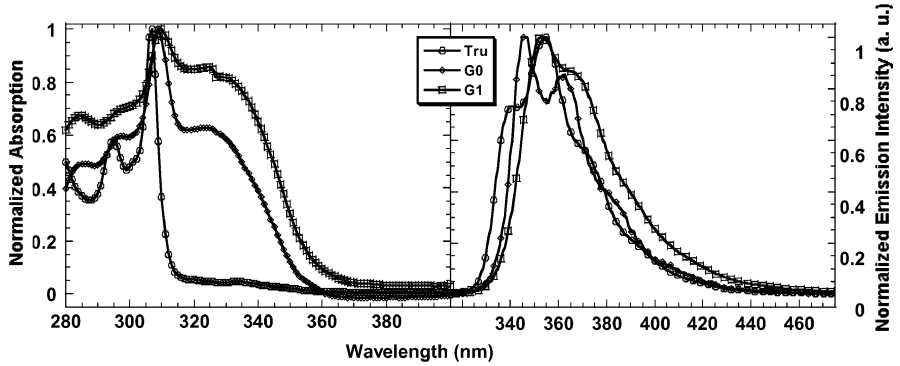

FIGURE 5. Absorption (left) and emission (right) spectra for dendrimers in THF solutions.

of chemically different nuclei is usually separated by using a different solvent.

Optical Properties. The absorption spectra for **1**, **G0**, and **G1** in THF solutions are shown in Figure 5. Normally, π-conjugated dendrimers show a very strong $\pi-\pi^*$ electron absorption band in the UV−vis region, which progressively red-shifted with increase of effective conjugation length. From absorption spectra in Figure 5, we observed that absorption λ_{max} (309 nm for **G0** and 310 nm for **G1**, respectively) exhibited a small red-shift with the increase of the truxene moiety and of the generation of the dendrimer in comparison with that of **1** (307 nm) by virtue of the large molar extinction coefficients ($\epsilon > 10^5$ M^{-1} cm^{-1}). However, absorption spectra showed very strong shoulder peaks at 320 nm for **G0** and 330 nm for **G1**, respectively, while the intensity of such peak of **G1** was higher than that of **G0**. We also observed that onsets of absorption spectra were obviously red-shifted from **1** to **G1**. The absorption λ_{max} for these compounds might belong to the $\pi-\pi^*$ electron absorption band of the truxene skeleton, and we did not observe the very obvious $\pi-\pi^*$ delocalization with the increase of the truxene moiety, which was owing to the large torsion angle between the benzene ring and the truxene system caused by three giant truxene skeletons at one smaller benzene ring. However, the intensity of shoulder peaks augmented from **G0** to **G1**, which suggested that the relative delocalization might be promoted with an increase of the generation of dendrimers.

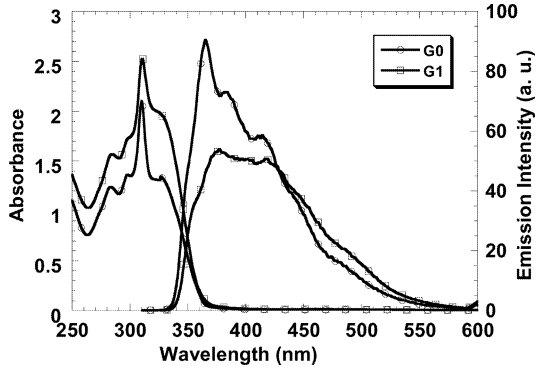

FIGURE 6. Absorption and photoluminescence spectra of **G0** and **G1** in solid states.

The optical absorptions of **1**, **G0**, and **G1** in the solid states are shown in Figure 6. The structured absorption bands observed in solution were also exhibited in the solid states. However, absorption peaks on the solid state were slightly red-shifted to their corresponding ones in solution. The similarity of absorption spectra shape on the solution and the solid state in these molecules suggested that there was a slight increase in conjugation length in the solid state, which indicated that the π-stacking in solid state was significantly reduced due to the giant truxene moiety and also because of the large torsion angle between the truxene group and the phenyl group. The intensity of shoulder peaks augmented from

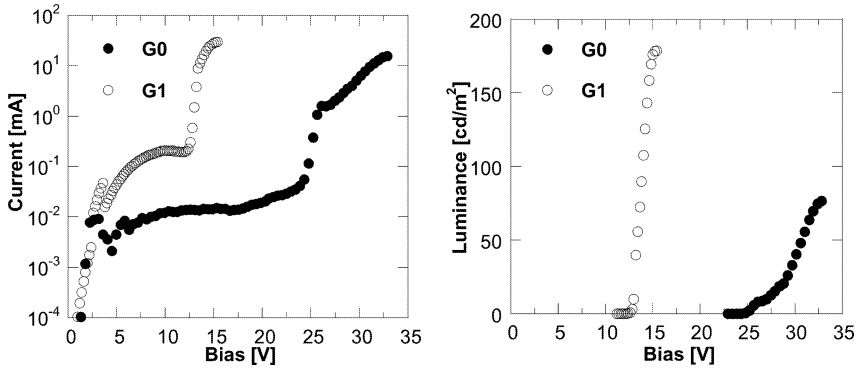

FIGURE 7. Current−voltage (a) and current−luminance characteristics of OLEDs with the following configuration: ITO/PEDOT/dendrimer **G0** or **G1**/Ba/Al.

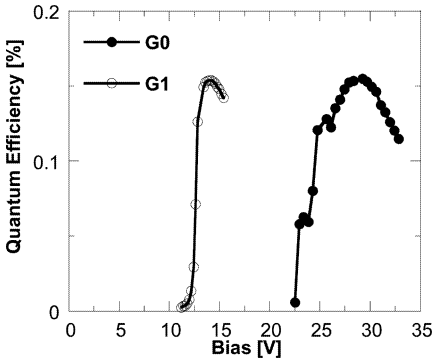

FIGURE 8. Comparison of external EL quantum efficiency of dendrimers **G0** and **G1**.

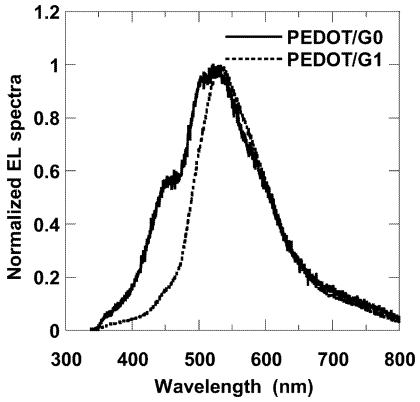

FIGURE 9. EL spectra of dendrimers **G0** and **G1**.

G0 to **G1**, which suggested that the relative delocalization might be promoted with an increase of the generation of dendrimers.

The photoluminescence (PL) spectra of **1**, **G0**, and **G1** in dilute solution (5×10^{-5} M) are also shown in Figure 5. All compounds have structured emission peaks. If the 0−0 transitions in the emission and corresponding absorption peaks were considered, the Stoke shift is small for these three compounds. In dilute solutions, no emission light was observed because the emission light of these three compounds was in the UV range. The PL spectra of **1**, **G0**, and **G1** in solid states are shown in Figure 6. In addition of their broad featureless characteristics, the emission spectra of these three compounds in the solid states slightly red-shifted from the dilute solution ones, which also indicated the decreased π-stacking in these molecules.

Organic Light-Emitting Properties. Some conjugated dendrimers have been used successively as charge-transporting layer in OLEDs due to their good charge-transporting characteristics and the fact that they can form stable amorphous films. We fabricated organic light-emitting diodes (OLEDs) from **G0** and **G1** as the emissive layer. Preliminary results on intrinsic electroluminescence (EL) of these dendrimers is first presented and discussed. Device configuration was: ITO/PEDOT/**G0** or **G1**/Ba/Al. Both the dendrimers emitted blue-green color at a forward bias (ITO wired positively) above 8 V. A typical curve of light intensity versus bias (L−V) is given in Figure 7. The external quantum efficiencies for **G1** and **G2** are compared in Figure 8. The external quantum efficiency (QE) was measure to be 0.16% at 27 V for **G0** and 0.16% at 13 V for **G1**, respectively. The EL spectra are also illustrated in Figure 9. In comparison with PL spectra in solid states (in Figure 6), it is obvious that EL emission is significantly red-shifted compared to that of PL spectra due to the formation of ketonic defects in the device processing.[16] The further improvement of the LED efficiency of these dendrimers can be achieved by modification of dendrimer/electrode interface in order to enhance and balance the electron and hole injection. The corresponding studies are in progress.

Conclusions

In conclusion, we have demonstrated a convenient and highly efficient convergent approach for the synthesis of a new family of large-size and precisely well-defined dendrimers and star-shaped molecules via "in-situ" generation of benzene core from aryl methyl ketones by acid-promoted cyclotrimerization reactions. We also have investigated their photophysical and electroluminescence. We have developed a platform to synthesize a new family of dendrimers utilizing giant polycyclic aromatics, further investigation toward the formation of hexasubstituted (briannulated) benzenoids using this strategy to create novel nonalternant polycyclic aromatic hydrocarbons containing alternating five- and six-membered rings are in progress. The unique NMR behaviors have exhibited

(16) (a) List, E. J. W.; Guentner, R.; de Freitas, P. S.; Scherf, U. *Adv. Mater.* **2002**, *14*, 374−378. (b) Gong, X.; Iyer, P. K.; Moses, D.; Bazan, G. C.; Heeger, A. J.; Xiao, S. S. *Adv. Funct. Mater.* **2003**, 325−330.

that the chemical shifts of the H-2′ of hexyl substituents move to the most upfield (0.48 ppm). The lowest energy calculations of the structure have proved that this methylene group is on the top of the shielding cone of polycyclic aromatic rings. The photoproperties of such dendrimers indicate that the large torsion angle between the giant truxene moiety and the benzene ring might affect full π-delocalization of the whole molecule. We have developed a platform to synthesize a new family of dendrimers utilizing giant polycyclic aromatics and to understand photophysical and electroluminescence properties of polycyclic dendrimers through the investigation of such dendrimers. The basic investigations with these macromolecules would provide novel insights and directions for the uses of novel extend π-conjugated dendrimers based on truxene in organic materials science. We expect that further investigation could also be devoted to the synthesis and characterization of nonalternating polycyclic aromatics.

Experimental Section

Basic Characterization. The NMR spectra were recorded at 298 K on a spectrometer operating at frequencies of 499.89 MHz (^{1}H) and 125.71 MHz (^{13}C) in $CDCl_3$, pyridine-d_5, and benzene-d_6 with concentrations of ~15 mg per 600 μL of solvent. Chemical shifts δ (ppm) were referenced to internal Me_4Si (TMS) for ^{1}H and solvent peaks for ^{13}C. Two-dimensional gradient-selected COSY (homonuclear correlated spectroscopy), HSQC (heteronuclear single quantum coherence), HMBC (heteronuclear multiple bond coherence), and ROESY (rotational NOE spectroscopy) experiments were performed using standard pulse sequences.

Device Fabrication and Characterization. LED was fabricated on pre-patterned indium−tin oxide (ITO) with sheet resistance 10−20Ω/□. The substrate was ultrasonic cleaned with acetone, detergent, deionized water, and 2-propanol. Oxygen plasma treatment was made for 10 min as the final step of substrate cleaning to improve the contact angle just before film coating. Onto the ITO glass was spin-coated a layer of polyethylenedioxythiophene-polystyrene sulfonic acid (PEDOT:PSS) film with thickness of 50 nm from its aqueous dispersion, aiming to improve the hole injection and to avoid the possibility of leakage. PEDOT:PSS film was dried at 80 °C for 2 h in the vacuum oven. The solution of dendrimer in *p*-xylene was prepared in a nitrogen-filled drybox and spin-coated on top of the ITO/PEDOT:PSS surface. Typical thickness of the emitting layer was 50−80 nm. Then a thin layer of barium as an electron injection cathode and the subsequent 200 nm thick aluminum protection layers were thermally deposited by vacuum evaporation through a mask at a base pressure below 2×10^{-4} Pa. The deposition speed and the thickness of the barium and aluminum layers were monitored by a thickness/rate meter. The cathode area defines the active area of the device. The typical active area of the devices in this study is 0.15 cm^2. The EL layer spin coating process and the device performance tests were carried out within a glovebox with nitrogen circulation. The luminance of the device was measured with a calibrated photodiode. External quantum efficiency was verified by the measurement of the integrating sphere, and luminance was calibrated after the encapsulation of devices with UV-curing epoxy and thin cover glass.

Acknowledgment. This work was supported by the Major State Basic Research Development Program (Nos. 2002CB613401 and 2002AA324080) from the Minister of Science and Technology and by the National Natural Science Foundation of China (NSFC 90201021 and 50103001).

Supporting Information Available: Complete experimental procedures; full characterization of all new compounds; NMR spectra. This material is available free of charge via the Internet at http://pubs.acs.org.

JO049268P